Energy 35 (2010) 729–739

Contents lists available at ScienceDirect

Energy

journal homepage: www.elsevier.com/locate/energy

A methodology of computation, design and optimization of solar Stirling power plant using hydrogen/oxygen fuel cells

Stoian Petrescu [a], Camelia Petre [a], Monica Costea [a,*], Octavian Malancioiu [a], Nicolae Boriaru [a], Alexandru Dobrovicescu [a], Michel Feidt [b], Charles Harman [c]

[a] Department of Engineering Thermodynamics, University POLITEHNICA of Bucharest, Splaiul Independentei, 313, 060042 Bucharest, Romania
[b] L.E.M.T.A., U.R.A. C.N.R.S. 7563, University "Henri Poincaré" of Nancy 1, 2 avenue de la Forêt de Haye, 54504 Vandoeuvre-les-Nancy, France
[c] Department of Mechanical Engineering, Duke University Durham, NC-27706, USA

ARTICLE INFO

Article history:
Received 31 October 2008
Received in revised form
21 August 2009
Accepted 28 October 2009
Available online 19 January 2010

Keywords:
Solar Stirling systems
Hydrogen
Fuel cell
Experimental data

ABSTRACT

The objective of this paper is to develop a methodology to determine how many houses could be fueled from the solar energy captured by a number of solar Stirling modules (with a fixed dish area per module) and also to determine the minimum necessary area of the fuel cell to ensure the amount of power needed to meet daily energy use requirements. The detailed method includes the effect of the fuel cell efficiency function on the power consumption of the user. Experimental data from our laboratory are used to determine the fuel cell efficiency as a function of the electric current density for a specific power demand. As an illustrative example, the analysis is applied to a residential area having a specific electrical demand. Using the developed method, the number of houses that could be fueled directly by the stored hydrogen is determined, and also the minim fuel cell area required.

© 2009 Elsevier Ltd. All rights reserved.

1. Introduction

Limited resources of fossil fuel, environmental problems regarding pollution and global warming, but most of all, the geopolitical dependence on crude oil are major challenges for our society. According to energy experts from all over the world, solar energy, fuel cell and hydrogen energy technologies will play an important role in the future energy economy [1–6]. They are now widely regarded as one of the key energy solutions for the 21st century [7–9]. In the recent years, fuel cell technologies have performed in some sectors such as military, industrial, space, portable, residential, transportation and trading [6,10].

When used in residential sector, uninterruptible energy is becoming necessary because of high standard of living, increasing of energy demand of residence. Therefore, there is a need for the systems which will provide required energy if the fuel cell is unconnected to grid and the systems will operate as reserve system when the fuel cell connect grid [11]. A fuel cell system worked by hydrogen can be used for the need. Otherwise, hydrogen energy utilization at residences is an alternative method especially for supply power demand of stationary or portable devices. While hydrogen can be generated using different technologies, only some of them are environmentally friendly. Thus, hydrogen generated from water using solar energy, solar-hydrogen, is a leading candidate for a renewable and environmentally safe energy carrier [12].

Research and development studies about fuel cells have been done increasingly. Efficiency models of a single fuel cell and fuel cell stack have been developed [10] in order to emphasize the factors that affect it. Also, the optimal operating conditions of a fuel cell system have been investigated based on empirical data and a generalized electrochemical semi-empirical model [4,13,14].

This paper presents advancement to our previously reported analytical model [15] for estimating the performance of a solar–electrolyser–fuel cell assembly to produce electric energy from solar energy. A scheme of computation, design and optimization of a solar Stirling power plant using hydrogen/oxygen fuel cells is presented. The proposed system is composed of two main parts: a combined solar-dish/receiver, Stirling engine and electric generator that transforms solar energy in electricity and a second part which operates when the electricity produced by the first part exceeds the household needs. It consists of an electrolyser generating hydrogen and storage tanks for the produced hydrogen. When solar radiation is missing or/and during the peak periods of electricity demand, fuel cells powered by the stored hydrogen are

* Corresponding author. Tel.: +40 21 4029405; fax: +40 21 3181001.
E-mail addresses: stoian.petrescu@yahoo.com (S. Petrescu), cameliapetre@yahoo.com (C. Petre), liana5802@yahoo.fr (M. Costea), michel.feidt@ensem.inpl-nancy.fr (M. Feidt), c.harman@duke.edu (C. Harman).

0360-5442/$ – see front matter © 2009 Elsevier Ltd. All rights reserved.
doi:10.1016/j.energy.2009.10.036

Nomenclature

A	area [m^2]
b	distance between wires (in regenerator) [m]
C	concentrator factor [–]
c_v	mass specific heat at constant volume [J kg^{-1} K^{-1}]
D	diameter [m]
d	wire screen diameter (in regenerator) [m]
E	solar insolation [W m^{-2}] or energy [J]
ΔG	Gibbs potential change [kJ $kmol^{-1}$]
H	hour angle
h	convective heat transfer coefficient [W m^{-2} K^{-1}]
I	current intensity [A]
k	thermal conductivity [W m^{-1} K^{-1}]
L	length [m]
m	mass [kg]
n_m	number of moles [kmol]
N_S	number of screens of the regenerator
n_r	revolution per minute [s^{-1}]
P	power [W]
p	pressure [Pa]
Δp	pressure loss [Pa]
Pr	Prandtl number [–]
$\dot{Q}$	heat transfer rate [W]
R	electrical resistance [Ω] or gas constant [J kg^{-1} K^{-1}]
S	piston stroke [m]
T	temperature [K]
U	current voltage [V]
V	volume [m^3]
w	piston speed [m s^{-1}]
$\overline{w}_{H_2}$	specific reversible electrical work in the fuel cell [kJ $kmol^{-1}$]
X	coefficient of regenerative losses
y	adjusting coefficient
Z	zenith angle
z'	adjusting coefficient

Greek symbols

α	global absorptivity
ε_m	receiver global emissivity
ε_v	volume ratio
γ	specific heat ratio
δ	declination angle or insulation depth [m]
Φ	northern latitude
η	efficiency
σ	Stefan–Boltzmann constant [W m^{-2} K^{-4}]
ν	viscosity of the working gas [m^2 s^{-1}]
τ	solar module operating period [s] or ratio of the gas extreme temperatures
$\tau_{M/E}$	time of day in the morning/evening consumption period, [h]

Subscripts

avail	refers to available
B	refers to the base consumption period
CC	refers to Carnot cycle
cav	refers to the receiver cavity
conc	refers to the concentrator
cpr	refers to the compressor electric storage energy consumption
EG	refers to the electrical generator
ef	refers to effective value
el	refers to electric
elect	refers to electrolyser
ext	refers to receiver external wall
FC	refers to fuel cell
g	refers to the gas
HE	refers to hydrogen to electric energy conversion
H, g	refers to the gas at the source
inst	refers to installation
int	refers to receiver internal wall or internal resistance
irrev	refers to irreversibility
L, g	refers to the gas at the sink
leakage	refers to hydrogen leakage from storage tanks
M/E	morning/evening
m	medium
max	maximum
min	minimum
mirr	refers to the mirror
nec	refers to necessary, required
R	refers to the regenerator
rec	refers to the receiver
S	refers to the Stirling engine
SE	refers to solar to electricity conversion
SEHE	acronym for Solar–Electricity–Hydrogen–Electricity
SL	refers to the sound speed, at sink temperature
SS	refers to solar system
tot	total
X	refers to regenerative losses
Δp	refers to pressure loss
II	refers to second law efficiency
1	refers to the initial state (at lowest pressure) of the Stirling cycle

used to produce electricity. A method for predicting the total efficiency and power output of solar Stirling engines was previously reported [16–19] and the results have proven to be highly accurate when compared to experimental data [20]. This method is improved here by considering the monthly variation of the solar radiation intensity [21,22], to simulate system operation during the whole year in any geographic location. The above-improved method was further enhanced by electrolyser and fuel cell performance calculations, based on a global system performance prediction. The improvements are made taking into consideration experimental data for the fuel cell efficiency. The analytical model of computation, introduced as SEHE scheme (Solar–Electricity–Hydrogen–Electricity), was previously reported [15] by considering constant fuel cell efficiency from the technical literature [23,24]. We note that the fuel cell efficiency decreases exactly at the peak electrical demand periods so considering a constant efficiency value for the fuel cell is not a proper choice for high accuracy calculations. The experiments done in our laboratory proved that the efficiency of the fuel cells is a variable function of the power consumption by the user and thus it should be introduced in the prediction model as an analytical function.

The objectives for this paper are: to present an innovative methodology for estimating the performances of a solar assembly to produce electricity by using hydrogen as an energy carrier, and to show that this methodology provides design elements for the system modules by taking into account variable solar insolation.

The practical example will show the effect of the semi-empirical relation for the fuel cell efficiency in the SEHE model when compared to the constant value previously used. Also, the number of houses that could be fueled by such a solar system and the

necessary minimum fuel cell area to cover the required energy demand will be determined.

The improvements to our SEHE scheme reflect important conclusions regarding the obtained results and the conditions needed to achieve a desired operating regime, as we shall see in what follows.

2. Recall of the SEHE scheme

2.1. The proposed system to be analyzed

Mainly, the considered system is composed by a solar module (solar energy concentrator, receiver, solar Stirling engine and an electric generator), electrolyser to produce hydrogen from water electrolysis, hydrogen storage tanks and fuel cells to produce electric energy using previously stored hydrogen. This system is presented in Fig. 1.

The solar module uses a solar Stirling engine to produce electric energy from concentrated solar radiation. This electric energy is directly used for covering domestic needs, the surplus fuelling an electrolyser that produces hydrogen from water electrolysis. The hydrogen is stored in special tanks as a compressed gas and used as an energy source. When electricity demands are higher than this direct supply, fuel cells are used to produce electricity from the stored hydrogen.

2.2. SEHE analytical model

This detailed model was developed taking into account that energy demand could be covered either directly from solar energy or by use of produced and stored hydrogen during peak electricity demands or cloudy days.

The performance of the solar module (total efficiency and electric power) is predicted by using a previously validated model based on the Direct Method [16] for the Stirling solar engine, coupled to solar dish–receiver efficiencies calculations.

The developed equations are based on the First Law of Thermodynamics for processes with finite speed that are integrated in such a manner that the expressions for efficiency and power output are obtained directly for any irreversible cycle. An important notice is that this analytical prediction gives us the opportunity to make the calculations at any solar insolation E. This is happening because the solar insolation E is one of the important variables of the analytical model and based on this, all the performances of the whole system (efficiency and power) are expressed as functions of it (E). In the technical literature, data referring to similar solar systems are also available but unfortunately only for certain values of the solar insolation (usually for maximum values of insolation E) [20].

2.2.1. Solar module calculation

The electric power produced from solar energy is given by:

$$P_{SE} = EA_{mirr}\,\eta_{conc}\eta_{rec}\eta_S\eta_{EG} = EA_{mirr}\,\eta_{tot} \tag{1}$$

where the mirror area is (see Fig. 2):

$$A_{mirr} = \frac{\pi D_{mirr}^2}{4} \tag{2}$$

By applying the First Law, the cylindrical cavity receiver efficiency is found a function of solar insolation, E, and other mirror parameters [25]:

$$\eta_{rec} = \alpha_{cav}\left[1 - \frac{\varepsilon_m}{\alpha_{cav}}\frac{\sigma T^4}{\eta_{mirr}\cdot E\cdot C} - \frac{A_{ext}\,h_{ext}(T_{ext}-T_0) + A_{int}\,h_{int}(T-T_0)}{\alpha_{cav}\cdot\eta_{mirr}\cdot E\cdot C\cdot A_{cav}}\right] \tag{3}$$

where the concentrator factor is:

$$C = \left(\frac{D_{mirr}}{D_{rec}}\right)^2 \tag{4}$$

The main areas of the concentrated solar receiver (in the focal point of the parabolic dish mirror) are computed from the geometric characteristics of it:

$$A_{ext} = \pi(D_{rec}+2\delta)\,(L_{rec}+\delta) \tag{5}$$

$$A_{int} = \pi D_{rec}L_{rec} + \frac{\pi D_{rec}^2}{4} \tag{6}$$

$$A_{cav} = \frac{\pi D_{rec}^2}{4} \tag{7}$$

Also, the external temperature T_{ext} of the wall of the receiver is computed with the formula:

$$T_{ext} = \frac{\frac{k}{\delta}A_m T + A_{ext}h_{ext}T_0}{\frac{k}{\delta}A_m + A_{ext}h_{ext}} \tag{8}$$

where

$$A_m = \frac{A_{int}+A_{ext}}{2} \tag{9}$$

In order to optimize the heat transfer process, the following condition is imposed: the rate at which heat is transferred to the

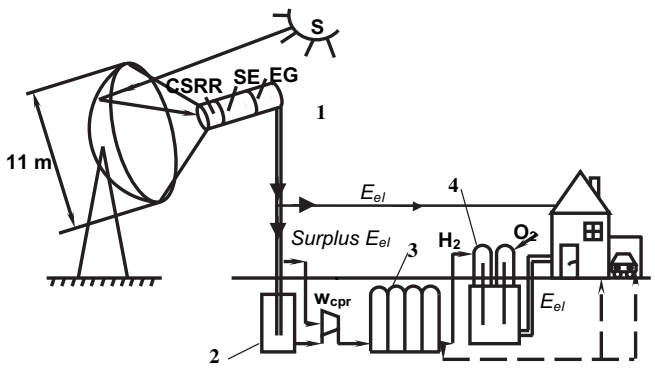

Fig. 1. Solar–electrolyser–fuel cell assembly: 1 – solar module with Stirling engine; 2 – electrolyser; 3 – hydrogen storage tanks; 4 – fuel cells [15].

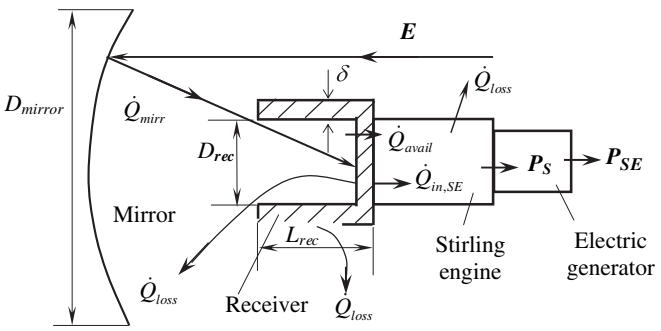

Fig. 2. The solar assembly: mirror–receiver–Stirling engine–electric generator.

engine equals the rate at which heat is received by the mirror times the receiver efficiency. By using Eq. (3), based on assuming a stationary state, this is:

$$\dot{Q}_{\text{avail}} = \eta_{\text{rec}} \cdot \dot{Q}_{\text{mirr}} = \eta_{\text{rec}} \cdot \eta_{\text{conc}} \cdot E \cdot A_{\text{mirr}} \tag{10}$$

providing that this rate of heat transfer is no more than the Stirling engine requires for operation at the particular piston speed.

Then, the optimum engine rotation speed should be:

$$n_{\text{r}} = \frac{60 \cdot \dot{Q}_{\text{avail}}}{z' m R T_{\text{H,g}} \ln \varepsilon_{\text{v}}} \tag{11}$$

where z' is one of the adjusting coefficients of the method with the value of 0.45. The numerical value of z' was determined on the basis of experimental data from operating solar Stirling engines [20] using their real operating parameters and conditions (geometrical parameters, thermodynamic ones and also for the solar insolation values).

Also, the Stirling engine efficiency η_S is computed as a function of available heat in the engine and thus, as a function of solar insolation. The Direct Method is used for this purpose, taking into consideration internal and external irreversibilities.

2.2.2. Stirling engine performance

The thermal efficiency of the Stirling engine is expressed as a product of the Carnot cycle efficiency and a second law efficiency [25–27], as has been suggested by Bejan [28]:

$$\eta_{\text{S}} = \eta_{\text{CC,g}} \cdot \eta_{\text{II,irrev}} = \left(1 - \frac{T_{\text{L,g}}}{T_{\text{H,g}}}\right) \cdot \eta_{\text{II,irrev}} \tag{12}$$

where the second law efficiency is given by:

$$\eta_{\text{II,irrev}} = \eta_{\text{II,X}} \cdot \eta_{\text{II,}\Delta p} \tag{13}$$

The losses accounted for in the above expression of the second law efficiency are those due to incomplete regeneration and pressure losses respectively.

Incomplete regeneration represents a major loss in Stirling engines. This loss is expressed by using a coefficient of regenerative losses, X. An analysis for determining this loss has been made [29]:

$$\eta_{\text{II,X}} = \frac{1}{1 + \dfrac{X \cdot c_{\text{v}}}{R \ln \varepsilon_{\text{v}}}\left(1 - \dfrac{T_{\text{L,g}}}{T_{\text{H,g}}}\right)} \tag{14}$$

with

$$X = X_1 \cdot y + X_2 \cdot (1 - y) \tag{15}$$

where y is the second adjusting coefficients of the method, and X_1, X_2 are regenerative losses coefficient values corresponding to an "optimistic", respectively "pessimistic" evaluation of them. The value of y has been determined from experimental data of 4 solar Stirling engines [16]. Setting $y = 0.27$ provided the best fit between analytical results and experimental one, so this value is used as an adjusting coefficient in the theoretical analysis.

In the above relation [29]:

$$X_1 = \frac{1 + 2M + \mathrm{e}^{-B}}{2(1 + M)} \tag{16}$$

$$X_2 = \frac{M + \mathrm{e}^{-B}}{1 + M} \tag{17}$$

$$M = \frac{m_{\text{g}} c_{\text{v,g}}}{m_{\text{R}} c_{\text{R}}} \tag{18}$$

$$X_2 = \frac{M + e^{-B}}{1 + M} \tag{19}$$

in which the convection coefficient h is computed as:

$$h = \frac{0.395(4p_{\text{m}}/RT_{\text{L,g}}) w^{0.424} c_p(T_{\text{m}}) \cdot \left[\nu(T_{\text{m}})\right]^{0.576}}{(1+\tau)\left[1 - \frac{\pi}{4[(b/d)+1]}\right] D_{\text{R}}^{0.576} \cdot Pr^{2/3}} \tag{20}$$

The expression of the second law efficiency due to pressure losses is [30]:

$$\eta_{II,\Delta p} = 1 - \frac{\frac{w}{w_{S,L}}\gamma\left(1+\tau^{1/2}\right)\ln\varepsilon_v + 5\left(\frac{w}{w_{S,L}}\right)^2 N_S}{\tau \cdot \eta_{CC} \cdot \eta_{II,X} \ln \varepsilon_v} - \frac{\frac{3(0.94+0.045w)10^5}{4p_1}}{\tau \cdot \eta_{CC} \cdot \eta_{II,X} \ln \varepsilon_v} \tag{21}$$

where the speed of sound is used:

$$w_{\text{S,L}} = \sqrt{\gamma R T_{\text{S,L}}} \tag{22}$$

and the pressure in state 1 is expressed as a function of the mean gas pressure:

$$p_1 = \frac{4p_m}{(\varepsilon_{\text{v}} + 1)(\tau + 1)} \tag{23}$$

where

$$\tau = \frac{T_{\text{H,g}}}{T_{\text{L,g}}} \tag{24}$$

$$\varepsilon_{\text{v}} = \frac{V_{\max}}{V_{\min}} \tag{25}$$

By expressing all these parameters as a function of the piston speed w, in fact we introduce the rotation speed n_{r} [rpm]:

$$w = 2 \cdot S \cdot n_{\text{r}}/60 \tag{26}$$

The above analysis shows that the pressure losses and their effect on efficiency and power output of the engine depend on the mean piston speed and hence the engine rotation speed.

This model was used to optimize a solar module and was validated for 4 solar engines [16,17] (see also Fig. 3 and Table 1) with experimental data [20] and further completed with the electrolyser and fuel cell calculations for the SEHE scheme [15]. Note that this technique for calculating the efficiency and power of Stirling engines has been validated by comparing the results predicted by such analysis with performance data taken on twelve actual Stirling engines over a range of sixteen operating regimes [18,19]. The high degree of correlation between the analytic and the operational data indicates that the analysis is capable of accurately predicting Stirling engine performance under a wide range of conditions.

2.2.3. Hourly solar insolation prediction

Regarding the solar insolation E, it is introduced in our model as an analytical prediction formula available on NASA site [21,22], as a function of clear day solar insolation on a surface perpendicular to incoming solar radiation and the Zenith angle, which depends on the latitude, solar declination angle and time of day through the hour angle.

In order to predict hourly solar insolation values to be used in our SEHE model, at different seasons and latitudes, we chose to use an analytical prediction formula available on NASA site [21]. It is

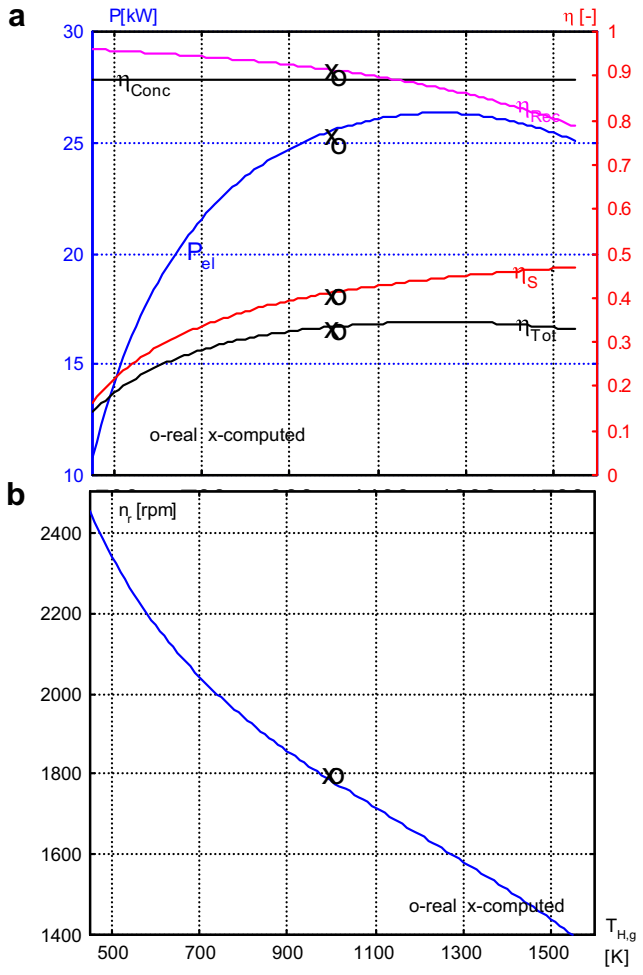

Fig. 3. Performance of the Vanguard combined Solar/Dish Stirling engine assembly [11], for emissivity = 0.87: a) Electrical power output (P_{el}) and efficiencies (η_{conc}, η_{rec}, η_S, η_{tot}) as a function of the gas temperature at the source; b) Rotation speed variation of the Stirling Engine with the gas temperature at the source.

known [31–33] the fact that for plane concentrators the diffuse insolation is important, while for dish concentrating receivers, due to the mirror surface properties having directional reflection, the fraction of diffuse insolation that could be concentrated in the focal point is neglected in comparison to the direct one. Since the solar Stirling engine assembly is composed of parabolic dish mirrors, we have considered in our model only direct insolation [21]:

$$E = E_0 \cos(Z) \tag{27}$$

where $E_0 \sim 1000\ \mathrm{W/m^2}$ represents the clear day solar insolation on a surface perpendicular to incoming solar radiation. This value actually varies greatly due to atmospheric variables;

$$Z = \arccos[\sin(\Phi)\sin(\delta) + \cos(\Phi)\cos(\delta)\cos(H)]$$

is the zenith angle (zenith angle is the angle from the zenith (point directly overhead) to the Sun's position in the sky). The zenith angle is dependent upon latitude Φ, solar declination angle δ, and time of day through the hour angle H:

$$H = 15^\circ \times (\mathrm{time} - 12) \tag{27a}$$

The hour angle is the angle of radiation due to time of day. Time is given in solar time as the hour of the day from midnight.

The solar declination angle δ for the northern hemisphere is given at different periods of the year:

Vernal Equinox March 21/22, $\delta = 0^\circ$ Autumnal Equinox September 21/22, $\delta = 0^\circ$

Summer Solstice June 21/22, $\delta = +23.5^\circ$ Winter Solstice December 21/22, $\delta = -23.5^\circ$

Thus, by using this analytical prediction for solar insolation and due to the fact that our validated solar Stirling model is function of this variable, we are able to make all calculations at different times of day, of year and latitudes.

2.2.4. Daily demand of electric energy per house

Considering an ordinary house, we propose the following daily electric energy demand, which is divided on four periods of the day, upon usual necessities:

a) a "base consumption" (24 h/day) should take into account:
   - a domestic refrigerator: 402 kWh/year;
   - a freezer: 307 kWh/year.
b) the "morning period" should contain the base consumption and:
   - an electric boiler: 1.5 kW;
   - a microwave oven: 1 kW;
   - a toaster: 0.8 kW;
   - a coffee machine: 0.75 kW;
   - a fruit juicer: 0.025 kW;
   - electric light: 3 bulbs of 0.1 kW each.

We suppose that the boiler operates for 30 min, the lightening for all morning period (3 h), the coffee machine for 1 h and all the other devices for 15 min;

Table 1
Numerical results for predicting the performances of solar Stirling engine assemblies.

Solar assembly		Receiver efficiency		Engine efficiency		Total efficiency		Electric Power		ε_m
		Real [%]	Analytic [%]	Real [%]	Analytic [%]	Real [%]	Analytic [%]	Real [kW]	Analytic [kW]	[–]
Vanguard	Op	90	92	41	41	32.84	33.26	25	25.4	0.87
	Max	90	87	–	44	–	34.48	–	26.33	
Vanguard	Op	90	93	41	42	32.84	34.25	25	26.15	0.3
	Max	90	88	–	46	–	36.3	–	27.71	
MDAC	Op	90	92	38–42	40	30–33	32.66	25	24.93	0.87
	Max	90	87	–	44	–	34.11	–	26.04	
MDAC	Op	90	93	38–42	41	30–33	33.56	25	25.62	0.3
	Max	90	88	–	46	–	35.91	–	27.42	
SBP 17	Op	80	78	42	40	26.44	24.54	50	48.74	0.87
	Max	80	78	–	40	–	24.54	–	48.75	
SBP 17	Op	80	80	42	42	26.44	26.26	50	52.16	0.3
	Max	80	79	–	42	–	26.29	–	52.22	

Op = operating regime; Max = analytic maximum regime.

c) the "day period" and the "night period" should contain only the base consumption as people are in the offices;
d) the "evening period" should contain the base consumption and:
- a personal computer or a TV: 0.25 kW;
- an electric boiler: 1.5 kW;
- a mixer: 0.25 kW;
- a kitchen robot: 0.7 kW;
- a dish machine: 1.05 kWh/cycle;
- a washing machine: 1.02 kWh/cycle;
- a microwave oven: 1 kW;
- electric light: 3 bulbs of 0.1 kW each;
- an air conditioning unit.

We suppose that the boiler operates for 80 min, the lightening for all evening period (5 h), the personal computer or/and the TV for 3 h and all the other cooking devices for 60 min and/or 1 cycle. Regarding the air conditioning unit, we have to differentiate the period of the year; thus we consider the cooling capacity of 1.25 kW in the summer time for 60 min and the heating load of 1.3 kW in the winter time for 5 h.

The electric energy demand is estimated using the above described consumptions by two sinusoidal curves that closely fit the measured data available at the Romanian National Institute of Statistics [34]. These two sinusoidal curves correspond to morning and evening pick demand periods, while during night the demand is considered constant for few hours. A similar consumption estimation curve was published in technical literature regarding Bulgaria, which is close to Romania, for which the study is presented [35].

The two sinusoidal parts of this estimation were built taking into account the pick value of the electric power demand and a time of day corresponding to the consumption considered period (M – morning, respectively E – evening), so that a smooth increase and decrease in demand are considered:

$$P_{M/E} = P_B + \frac{\left(P_{M/E,max} - P_B\right)}{2}\left[1 + \sin\left(\tau_{M/E}\cdot\frac{2\pi}{d_{M/E}} - \frac{\pi}{2}\right)\right] \quad (28)$$

where P_B is the power on the base consumption period, $P_{M/E,max}$ is the pick (maximum) power on the morning, respectively evening period, $d_{M/E}$ is the total pick duration for the morning (M subscript), respectively evening (E subscript).

The above relation has been determined based on the equivalence of the area defined by the sinusoidal curve with x axis and the energy consumption computed by summing all operating devises on the considered time interval, as equivalent energies.

2.2.5. Assembly

Briefly, the total electric energy produced by the assembly of operating solar modules

$$E_{inst} = N_{modules} P_{SE} \tau_{SS} \text{ [kJ]} \quad (29)$$

is compared to the total electric energy demand, which was estimated for a number of consumers (here, domestic residences) by accounting for various items of domestic equipment

$$E_{el,nec,tot} = N_{houses} E_{el,nec} \text{ [kJ]} \quad (30)$$

where the hourly electric energy necessary for a house, $E_{el,nec}$, is the sum of the electric consumption of all units, for different periods of a day (nighttime, for which a base type consumption was considered, morning with a different consumption, noon and evening periods) estimated as described in section 2.2.4 and presented in Fig. 11.

The difference between them gives us the information about the periods on which we could produce H_2 or those on which we should use the stored H_2 to cover the electricity demand:

$$E_{inst} - E_{el,nec,tot} \begin{cases} > 0, & \text{surplus} \Rightarrow H_2 \text{ is produced} \\ < 0, & \text{deficit} \Rightarrow \text{stored } H_2 \text{ is used} \end{cases}$$

During surplus electric energy periods, the surplus electricity is used in an electrolyser to produce H_2. Taking into account the electrolyser efficiency η_{elect} (about 50% for common electrolysers), we were able to predict the quantity of produced H_2 $n_{M,H_2} = \eta_{elect} E_{el,surplus} / \overline{w}_{H_2,max}$ [kmol] and stored as a compressed gas at 200 bar (for which the specific energy consumption is $w_{cpr} = 0.47$ KWh/kg H_2). Note that $\overline{w}_{H_2,max}$ represents the maximum specific electrical work developed in a reversible electrochemical reaction in the fuel cell, at constant temperature and pressure. Its value is equal to $\Delta G = 237.18$ kJ/kmol. Thus the total amount of energy available later from the stored H_2, taking into account also a storage efficiency of about 98.8% (m_{H_2} leakages $= 1.2\% \times m_{H_2}$) is:

$$E_{H_2} = \frac{m_{H_2} - m_{H_2\ leakage}}{M_{H_2}} \overline{w}_{H_2,max} \text{ [kJ]} \quad (31)$$

On the other hand, during the periods on which the demand is higher than the supply, the deficit must be covered by using the produced and stored H_2 in a fuel cell. Up to now, we took into account a constant efficiency of the fuel cell (53% for ordinary fuel cells [36]), so that the electric energy obtained was:

$$E_{el,FC} = \eta_{FC} E_{H_2} \text{ [kJ]} \quad (32)$$

and the electric energy available to the consumer was obtained by subtracting from this the energy consumed by the storing process.

In order to complete all the above calculations and to add some sensitivity studies a special program using MATLAB software was created.

2.3. Obtained results

The previously obtained results show the different behavior of such a system in any geographic locations and also during a day period.

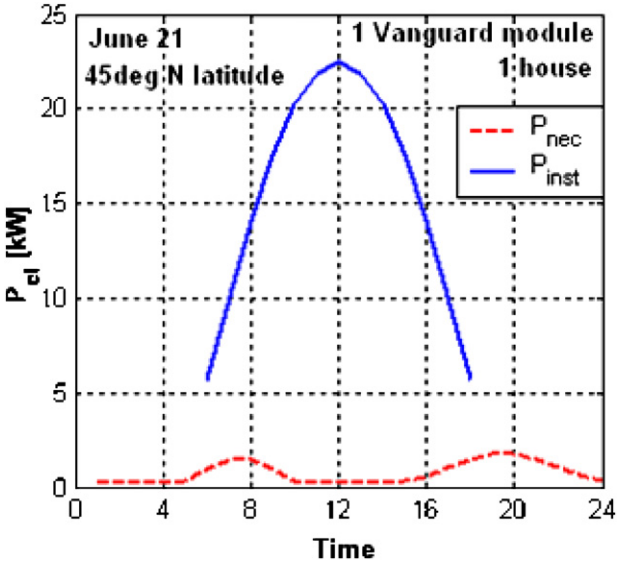

Fig. 4. Electric power supply and demand at June 21st (RO).

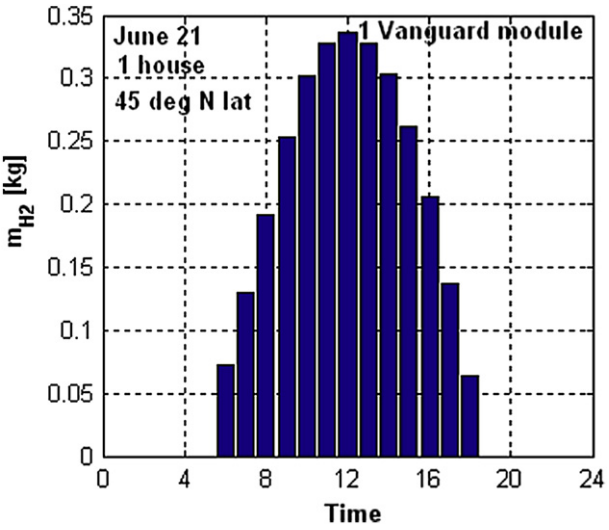

Fig. 5. Mass of produced H_2 at June 21st (RO).

For example, by integrating the curves represented in Fig. 4, we obtain the electric energy demand and supply for a house in Romania, in the summer time, when a solar Vanguard module [20] is operating.

During the surplus period (here, from around 7am–6pm), the mass of produced H_2 is represented in Fig. 5. As a comparison, Fig. 6 represents also the mass of produced H_2, but at March 21st. The magnitude and also the time interval are to be compared.

Other sensitivity studies were developed, such as: geographical location, number of consumers, number of operating solar modules, different types of solar modules.

3. Experimental results

3.1. Experimental equipment

The laboratory equipment that we used is composed of a photovoltaic panel, electrolyser, PEM fuel cell, hydrogen and oxygen reservoirs, voltmeter, amperemeter, electrical resistances, as seen in Fig. 7 [37]. The photovoltaic panel was used just to produce the hydrogen required for the fuel cell operation. From the fuel cell operation point of view, it does not matter where from this hydrogen is produced (photovoltaic panel or solar Stirling engine).

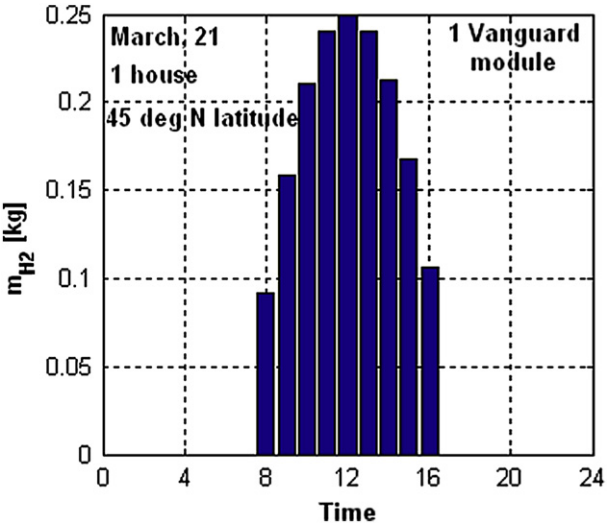

Fig. 6. Mass of produced H_2 at March 21st (RO).

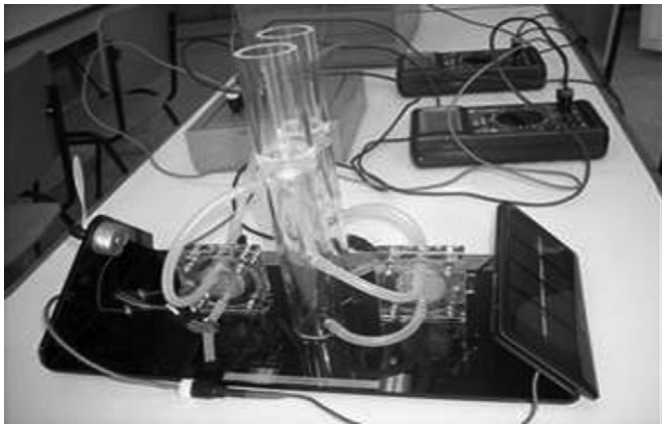

Fig. 7. Laboratory fuel cell installation [38].

Different electrical schemes could be arranged [37]. This possibility allowed us to get the electric voltage–current intensity characteristics for each component, as seen in Figs. 8 and 9.

More experimental data sets were measured, for accuracy.

3.2. Real performance of the fuel cell

Based on the measured values, we obtained the useful power (to consumer). For this, we established the internal resistance of the fuel cell circuit:

$$R_{\text{int}} = \frac{U}{I} - R \ [\Omega] \tag{33}$$

from an experimental set of data, when the resistance introduced in the circuit was zero. Its value was found to be $R_{\text{int}} = 5.8312\ \Omega$.

The useful power delivered by the fuel cell to consumer is:

$$P_{\text{useful}} = P - R_{\text{int}} \cdot I^2 \ [\text{W}] \tag{34}$$

where P is computed as the product between the electric current voltage and intensity.

The ohmic voltage drop is determined to be:

$$\Delta U_{\text{ohm}} = R_{\text{int}} \cdot I \ [\text{V}] \tag{35}$$

resulting the effective voltage

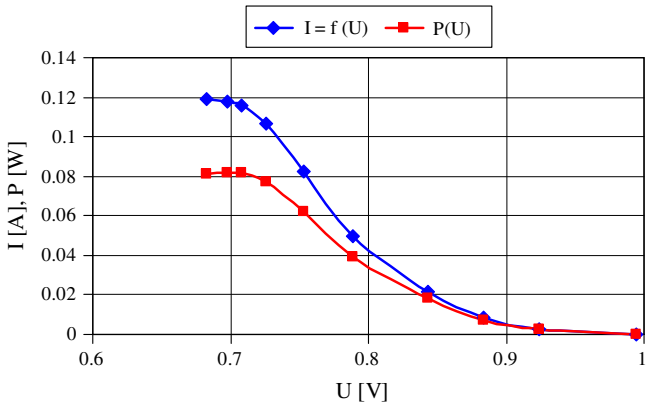

Fig. 8. Fuel cell electric current voltage–intensity characteristic.

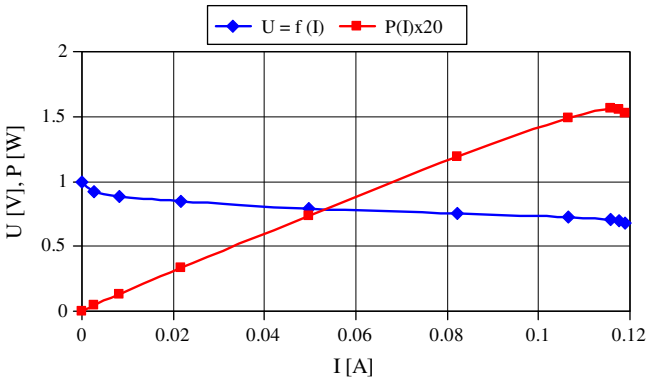

Fig. 9. Fuel cell electric current intensity–voltage characteristic.

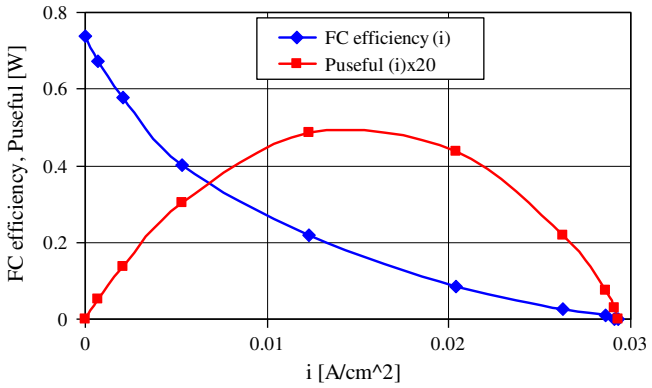

Fig. 10. Fuel cell useful power–current density and efficiency–current density characteristics.

$$U_{ef} = U - \Delta U_{ohm} \ [V] \tag{36}$$

and respectively the fuel cell efficiency:

$$\eta = \frac{U_{ef}}{U_0} \ [-] \tag{37}$$

where $U_0 = 1.23$ V represents the open circuit voltage [24].

It is very well known that U_0 can be computed from the Gibbs potential as $U_0 = \Delta G/nF$, where ΔG is the Gibbs potential change in the time of electrochemical reversible reaction in the fuel cell, n is the number of electrons involved in the reaction, F is the Faraday constant.

In a similar way U_{ef} can be expressed as function of Gibbs potential change in the irreversible process which takes place with a finite density of current i: $U_{ef} = \Delta G_{irr}/nF$. Replacing these two expressions in Eq. (37) we get a definition of the fuel cell efficiency expressed as function of energies, because ΔG represents how much electrical work is developed in the fuel cell in the time of reaction, reversible and respectively irreversible. Based on this consideration Eq. (32) is equivalent with Eq. (37).

It is very well known that in any irreversible process the efficiency will decrease in comparison with reversible processes. As a consequence, because of the three types of irreversibilities generated by activation overpotential, ohmic overpotential and concentration overpotential ΔG_{irr} will decrease as the density of the current i will increase. Which means that the U–I curve will be always decreasing with the increase of density of the current i. This means that the efficiency of the fuel cell will decrease with the increase of i. On the other side because the real power of the fuel cell is equal with the product between U_{ef} and I, the power of the fuel cell will increase first, towards a certain maximum value (optimum from the power point of view), will attain that maximum and after that will decrease as I will continue to increase. Of course that part of the curve is supposed not to be used because in that domain both performances will decrease (the efficiency and power).

So, the following fuel cell characteristics were built: useful power – current density to determine the maximum power operating regime, and also fuel cell efficiency – current density to determine the economic operating regime – Fig. 10.

By introducing this characteristic in our model, we are able to predict the real performance of the fuel cell.

This procedure allows us to predict the real fuel cell efficiency as a function of the electric current density by using an empirical equation determined from experimental data.

The empirical equation determined from the experimental fuel cell characteristics (Fig. 10) was determined as a function of the electric power to consumer:

$$\eta_{FC} = -21.33P_{FC} + 0.7303 \tag{38}$$

where the fuel cell power P_{FC} is determined as a function of the electric power demand, $P_{el,nec}$ (necessary to consumer – see Fig. 4), the available fuel cell area, A_{FC} (whose numerical value is considered here the one from our experiments, namely 4 cm^2) and the minimum necessary fuel cell area (for dimensioning application – see the explanations from section 4.1):

$$P_{FC} = \frac{P_{el,nec}}{A_{min}} A_{FC} \tag{39}$$

Thus, the fuel cell efficiency (relation (38)), that is to be introduced in the previously detailed computation scheme, is the experimental one.

4. Dimensioning calculations

4.1. From electric demand to "just necessary" number of fuel cells to be used

The presented computation SEHE scheme is applied to dimensioning calculations, determining the minimum fuel cells area (and implicitly the number of fuel cells of a known type and dimension) to be used in order to meet the electric energy demand to the consumer. Also, for the stated numerical application case, the number of consumers (houses) that could be directly fueled is determined.

The dimensioning algorithm is the following: estimating the maximum electric power demand, $P_{max,el,nec}$, for the four considered daily time intervals (maximum value from Fig. 12) and also the maximum fuel cells power, $P_{max,FC}$ (determined to be 0.025 W for the available fuel cell – see Fig. 10), we determine the minimum fuel cells area, A_{min}, to cover this maximum demand:

$$A_{min} = \frac{P_{max,el,nec}}{P_{max,FC}/A_{FC}} \left[m^2\right] \tag{40}$$

This value is used to compute the fuel cell power variation during a day, P_{FC} (Eq. (39)) and respectively, the fuel cell efficiency variation, η_{FC} (Eq. (38)).

Estimating the hour-by-hour electric energy consumption for one house, we determine the number of houses that could be fueled on these four time intervals, as a function of demand.

For this dimensioning calculation it is considered that all "minimum number" of fuel cells operate all the day, but at different powers and efficiencies.

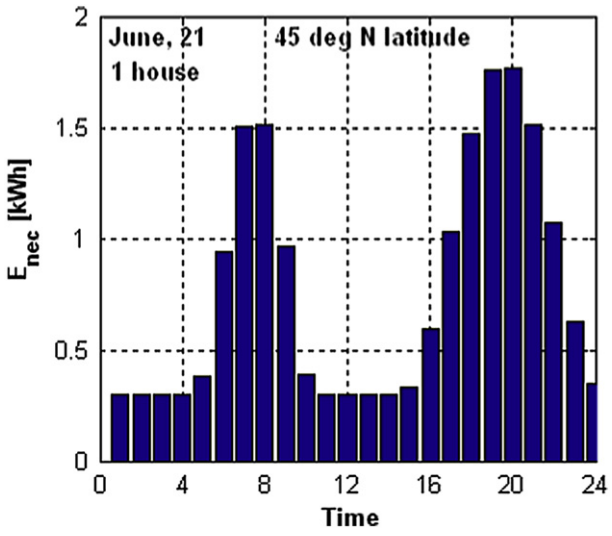

Fig. 11. Electric energy demand for one house, 24 h time interval, Romania geographic location, in the summer time.

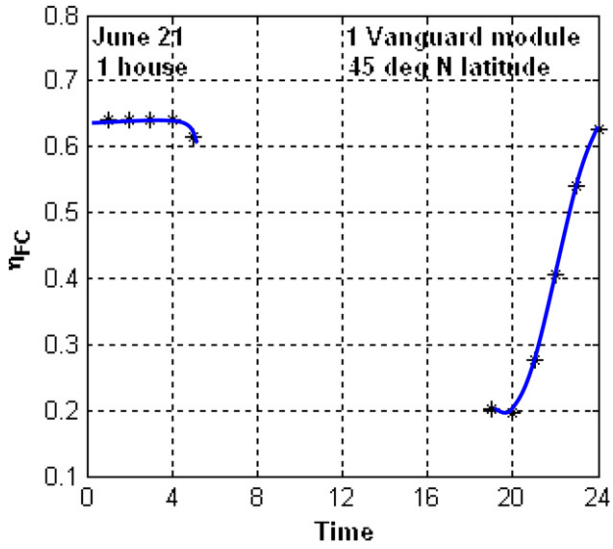

Fig. 13. Fuel cell efficiency as a function of time and electric power demand (summer time, Romania), only on the operating time period of the fuel cell.

5. Results

The electric energy demand for a house is estimated, during a day, by considering different electric devices operating on a specific period of time. This is shown in Fig. 11. The corresponding electric power demand is shown in Fig. 12, and is characterized by two peak demands in the morning and evening, respectively (for a residential consumer). A sinusoidal expression was established for the power consumption in order to model it analytically (Eq. (28)). By using this equation the fuel cell efficiency variations was obtained as shown in Fig. 13. The fuel cell operates only during the periods of electric energy "deficit", i.e. when solar energy is not enough to cover the electricity demand. This is why the values for the fuel cell efficiency were computed only on that two periods of time, in the morning and respectively in the evening, as it is represented in Fig. 13. It is to be noticed that the fuel cell efficiency decreases exactly at the peak electricity demand periods, so calculations based on constant efficiency are not appropriate for producing high accuracy results for a reliable design. A comparison of numerical results is also provided hereafter in order to show how much the difference between the two computation methods (with variable efficiency of the fuel cell versus the case of considering a constant efficiency of the fuel cell) could be.

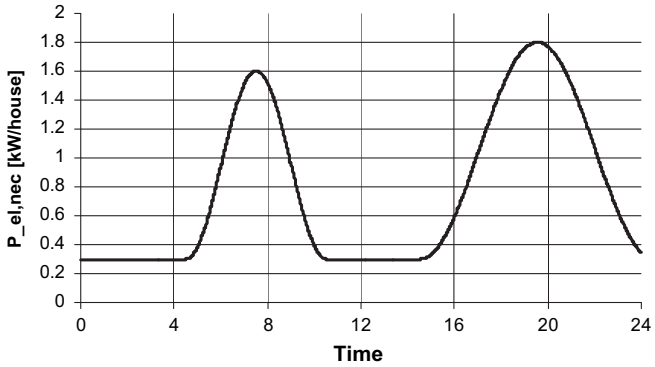

Fig. 12. Electric power demand for one house, 24 h time interval, Romania geographic location, in the summer time.

A global calculation leads to the following numerical result for a Vanguard type solar module [20] operating in the summer time in Romania (just as an example). It produces 2.9 kg H_2 daily, on a full shiny day. This represents 94.74 kWh after storing it as compressed gas in special tanks (i.e. after consideration of all losses corresponding to storage process: compression mechanical work, leakage, etc). This quantity of hydrogen is produced on the periods of electric energy "surplus", i.e. on the periods when the electric power coming directly from the solar Stirling engine is greater than the electric power demand. A direct feed of 9.93 kWh is insured on this period. The rest of electrical energy in surplus is used for producing hydrogen in an electrolyser which is stored and used later when the demand exceeds this direct supply. The deficit computed for this case (one house consumption during a summer day in Romania) is 8.66 kWh (1.58 kWh in the morning and 7.08 kWh in the evening and during night).

As a whole day balance: the daily deficit is 8.66 kWh, and could be covered by using the hydrogen produced 1 day before (which represents 94.74 kWh). The difference after covering the daily demand represents 1.93 kg hydrogen that is stored for cloudy days (equivalent electric energy of 86.08 kWh).

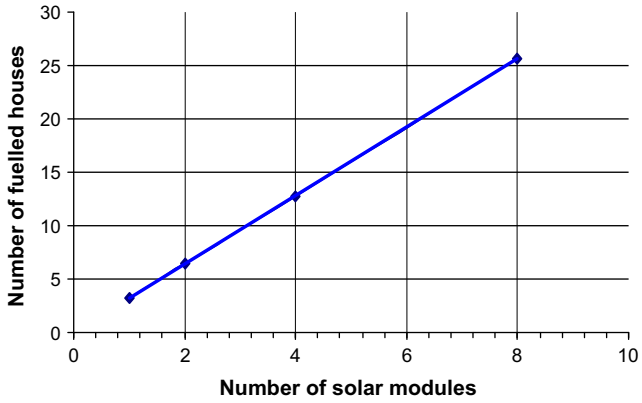

Fig. 14. Number of houses that could be fueled with electricity as a function of the number of operating solar modules, for a geographic location at 45°N latitude, with 365 sunny days yearly.

Taking into account this balance and a hypothetical month of 30 full sunny days, four houses could be fueled directly and by using the hydrogen stored during the previous day. By extrapolation to a different number of solar modules, Fig. 14 is obtained.

The same balance was also done by considering the entire summer season with cloudy days too, as reported in the Romanian official meteorological data [38], namely 39 sunny days and respectively 53 cloudy days (on the three summer months). At the end of the season, after covering all the demand for one house, 17.66 kg of hydrogen remains stored (for use during autumn, for example). This means that a module can cover the demand of only one house in the hypothesis of full solar electric energy feed (no other electric energy supply).

Comparing to the case of considering constant fuel cell efficiency (a value of 0.53 was considered [36]), it results that a quantity of 2.39 kg of hydrogen is stored at the end of a day, in comparison to the above result of 1.93 kg. Thus, considering constant fuel cell efficiency, an overestimation of the remaining quantity of hydrogen appears (0.46 kg/day).

Also regarding the numerical results, the minimum fuel cell area (determined from Eq. (40)) is 29 m^2. This could be produced for example with a stack of 29 fuel cells, each 1 m^2 in area, stacked vertically and connected in series.

6. Conclusions

The objective of this approach was to develop and provide a methodology of computation, design and optimization of solar Stirling power systems completed with electrolyser and fuel cells. The methodology closely simulates the operation of such systems with insight to the mechanisms that generate the irreversibilities in the Stirling engine, introduces the fuel cell efficiency as a function of the electric power to consumer allowing dimensioning calculations and optimization of the system design.

An important advantage of this methodology consists of considering the solar insolation E, as a function of clear day solar insolation on a surface perpendicular to incoming solar radiation and the zenith angle. Thus, it depends on the latitude, solar declination angle and time of day through the hour angle, and has applicability at any times of the day, year and at any latitude on earth.

As the paper presents a methodology, the following short revision is required as an algorithm to be followed:

1. Hourly solar insolation is predicted for the desired geographic location and season: Eq. (27).
2. Performances of Stirling solar module are computed: Eqs. (1) and (12). Then, the total installed electric energy is computed: Eq. (29).
3. Hourly electric energy demand is predicted for the consumer: section 2.2.4. The total electric energy demand is computed: Eq. (30).
4. The quantity of electricity direct supply and produced hydrogen is calculated as presented in section 2.2.5.
5. For estimating the fuel cell efficiency formula, one should:
   - take the electric voltage–current intensity characteristic of the fuel cell, from the fuel cell trader, as seen in Figs. 8 and 9;
   - compute the effective voltage: Eq. (36);
   - compute the fuel cell efficiency: Eq. (37);
   - build the useful power–current density and the fuel cell efficiency–current density characteristics (as seen in Fig. 10) in order to determine the maximum power of the fuel cell and to establish the dependence of fuel cell efficiency on electric power of the fuel cell, as Eq. (38);
   - determine the minimum required area of fuel cells: Eq. (40), in order to cover the electric energy demand with the available fuel cell module. Also the number of fuel cell modules can be easily determined;
   - calculate the power that is to be assured by the fuel cell modules: Eq. (39), and respectively the fuel cell efficiency function on this power: Eq. (38).

This fuel cell efficiency formula is used in the SEHE model to compute the electric energy needed to cover the deficit to consumer Eq. (32), implicitly the consumption of stored hydrogen required to cover this deficit of electric energy. A whole balance could be built now.

As perspectives, we intend to make a whole year simulation, for different users. We appreciate that the subject is of very high interest nowadays and we are sure that developments in this field will produce more efficient and economically viable systems.

Acknowledgements

The authors wish to thank the reviewers for their careful, equitable and constructive suggestions, which led to this revised manuscript.

References

[1] Lund H. Renewable energy strategies for sustainable development. Energy 2007;32(6):912–9.
[2] Barbir F. Transition to renewable energy systems with hydrogen as an energy carrier. Energy 2009;34(3):308–12.
[3] Schäfer A, Heywood JB, Weiss MA. Future fuel cell and internal combustion engine automobile technologies: a 25-year life cycle and fleet impact assessment. Energy 2006;31(12):2064–87.
[4] Shapiro D, Duffy J, Kimble M, Pien M. Solar-powered regenerative PEM electrolyzer/fuel cell system. Solar Energy 2005;79(5):544–50.
[5] Chaparro AM, Soler J, Escudero MJ, de Ceballos EML, Wittstadt U, Daza L. Data results and operational experience with a solar hydrogen system. Journal of Power Sources 2005;144(1):165–9.
[6] Solar-hydrogen power system for the Caymans. Fuel Cells Bulletin 2007; 2007(8):9–10.
[7] Brown JE, Hendry CN, Harborne P. An emerging market in fuel cells? Residential combined heat and power in four countries. Energy and Policy 2007;35(4):2173–86.
[8] Edwards PP, Kuznetsov VL, David WIF, Brandon NP. Hydrogen and fuel cells: towards a sustainable energy future. Energy and Policy 2008;36(12):4356–62.
[9] Neef HJ. International overview of hydrogen and fuel cell research. Energy 2009;34(3):327–33.
[10] Hou Yongping, Zhuang Mingxi, Wan Gang. The analysis for the efficiency properties of the fuel cell engine. Renewable Energy 2007;32(7):1175–86.
[11] Lund H, Duić N, Krajačić G, Carvalho MdG. Two energy system analysis models: a comparison of methodologies and results. Energy 2007;32(6):948–54.
[12] Perry S, Klemeš J, Bulatov I. Integrating waste and renewable energy to reduce the carbon footprint of locally integrated energy sectors. Energy 2008;33(10): 1489–97.
[13] Wishart J, Dong Z, Secanell M. Optimization of a PEM fuel cell system based on empirical data and a generalized electrochemical semi-empirical model. Journal of Power Sources 2006;161(2):1041–55.
[14] Martins LS, Gardolinski JEFC, Vargas JVC, Ordonez JC, Amico SC, Forte MMC. The experimental validation of a simplified PEMFC simulation model for design and optimization purposes. Applied Thermal Engineering 2009; 29(14–15):3036–48.
[15] Petrescu S, Petre C, Costea M, Malancioiu O, Boriaru N, Dobrovicescu A, et al. Performance analysis of solar Stirling systems generating hydrogen and electricity. In: ECOS'07-20th international conference on efficiency, cost, optimization, simulation and environmental impact of energy systems, Padova, Italy; 2007. p. 27–34.
[16] Petrescu S, Harman C, Costea M, Popescu G, Petre C, Florea T. Analysis and optimization of solar-Dish/Stirling engines. In: 31st ASES annual conference, SOLAR 2002 on sunrise on the reliable energy economy, Reno, Nevada, USA; 2002.
[17] Petrescu S, Harman C, Costea M, Florea T, Petre C, Feidt M. A scheme of computation, analysis, design and optimization of solar Stirling engines. In: Houbak N, editor. ECOS'2003-16th Int. conference on efficiency, cost, optimization, simulation and environmental impact of energy systems, Copenhagen, Denmark, vol. 3. p. 1255–62.

[18] Petrescu S, Costea M, Harman C, Florea T. Application of the direct method to irreversible Stirling cycles with finite speed. International Journal of Energy Research 2002;26:589–609.
[19] Florea T, Petrescu S, Florea E. Schemes for computation and study of irreversible processes in Stirling engines. [Scheme de calcul si studiu al proceselor ireversibile din motoarele Stirling]. Constanta: Leda & Muntenia; 2000 [in Romanian].
[20] Stine WB, Diver RB. A Compendium of solar Dish/Stirling technology. Sandia Laboratories Report, SAND93-7026 UC-236; 1994.
[21] Feidt M, Costea M, Petre C, Boussehain R. Génie énergétique appliqué au solaire. Energie solaire thermique. Bucharest: Printech; 2004.
[22] NASA. Relating solar radiation physics to earth & space science concept. Available at: http://education.gsfc.nasa.gov/experimental/all98invProject.Site/Pages/science-briefs/ed-stickler/ed-irradiance.html.
[23] Mugerwa MN, Blomen LJMJ. Fuel cell system economics. In: Blomen LJMJ, Mugerwa MN, editors. Fuel cell systems. New York: Plenum Press; 1993.
[24] Laramie J, Dicks A. Fuel cell systems explained. Chichester: John Wiley & Sons; 2000.
[25] Costea M. Improvement of heat exchangers performance in view of the thermodynamic optimization of Stirling machine. Unsteady-state heat transfer in porous media. Ph.D. thesis, University POLITEHNICA Bucharest & University Henri Poincaré Nancy 1; 1997. see also: http://cat.inist.fr/?aModele=afficheN%26cpsidt%3d183560.
[26] Petrescu S, Zaiser J, Petrescu V. Lectures on advanced energy conversion. Lewisburg, PA, USA: Bucknell University; 1996.
[27] Costea M, Petrescu S, Harman C. The effect of irreversibilities on solar Stirling engine cycle performance. Energy Conversion & Management 1999;40:1723–31.
[28] Bejan A. Advanced engineering thermodynamics. New York: John Wiley and Sons Inc.; 1988.
[29] Petrescu S, Florea T, Harman C, Costea M. A method for calculating the coefficient for the regenerative losses in Stirling Machines. In: The 5th European Stirling forum 2000, Ösnabruck, Germany; 2000. p. 121–9.
[30] Petrescu S, Costea M, Harman C, Florea T. Determination of the pressure losses in a Stirling cycle through use of a PV/Px diagram. In: Hirs GG, editor. ECOS'2000-Inter. sympos. on efficiency, costs, optimization simulation and environmental aspects of energy systems, Enschede, Netherlands; 2000. p. 659–70. See also: http://pcs.isiknowledge.com/uml/uml_view.cgi.
[31] Dănescu Al, Bucurenciu S, Petrescu S. Use of solar energy. [Utilizarea energiei solare]. Bucuresti: Ed. Tehnica 1980 [in Romanian].
[32] Duffy JA, Bekman WA. Solar energy thermal process. New York: John Wiley & Sons; 1974.
[33] Cengel Yunus A. Heat transfer. A practical approach. New York: Mc. Graw-Hill Companies Inc.; 2003.
[34] Romanian National Institute of Statistics. Energy residential consumption [Consumul casnic de energie]; January 1998 [in Romanian].
[35] Yaneva N, Welinov K. Investigation of the electricity consumption for lighting in the residential sector in Bulgaria. Right Light 4, 1997;2.
[36] Ballard's next generation heavy-duty fuel cell module; Mark1020 ACS, www.ballard.com.
[37] Hydrogen energy systems h-tec experiments – fuel cell, laboratory handbook. see also: www.h-tec.com.
[38] STAS 6648/2–82 State standard, official edition, exterior climate parameters; 1982 [in Romanian].